General Relativity and Gravitation, Vol. 18, No. 11, 1986

Einstein–Rosen Metrics Generated by the Inverse Scattering Transform[1]

Xavier Fustero[2] and Enric Verdaguer[2]

Received July 30, 1984

The most general Einstein–Rosen solutions obtainable by the inverse scattering transform, using the Levi-Cività metric as seed are analyzed. They can be classified as a family of evolving metrics without a clear physical interpretation and a family representing gravitational waves absorbed and radiated by a massive cylinder. The physical interpretation is based on a perturbative analysis, which shows that the solition waves have a peculiar superluminal effect, on the evaluation of the optical scalars and on Thorne's C energy.

1. INTRODUCTION

This paper deals with axisymmetric solutions of Einstein's equations. The nonasymptotic flatness of these metrics makes them of little use for the study of astrophysical or any realistic objects. However, they are the simplest metrics for which exact gravitational wave solutions are known. Their interest lies in the fact that they allow one to study exact properties of gravitational waves and that, one hopes, more realistic models of gravitational waves will share many of those properties. For this reason cylindrical symmetric solutions have been investigated extensively by many authors [1–3].

In recent years generating techniques have been developed to find solutions of Einstein's equations. Among them, there is the inverse scattering technique [4, 5] (Solition technique) that can be applied to

[1] Work partially supported by research project CAICYT no. 0534/81.

[2] Departament de Física Teòrica, Universitat Autònoma de Barcelona, Bellaterra (Barcelona), Spain.

0001-7701/86/1100-1141$05.00/0

metrics with two commuting Killing vectors. Vacuum solutions with almost arbitrary complexity can be generated by such a technique.

In this paper we analyze the solutions with cylindrical symmetry that can be generated this way. For simplicity we shall consider diagonal metrics only (Einstein–Rosen metrics), that is, hypersurface orthogonal Killing vectors. Those metrics can be seen as a limiting case of the more general nondiagonal metrics from which they can be obtained by a continuous parameter transformation [6]. This is an important point because Einstein's equations for the Einstein–Rosen metrics reduce to a linear equation plus a system solvable by quadratures, whereas the nondiagonal case is truly nonlinear. Therefore the diagonal solutions exhibited here can be expected to have a soliton-like behavior which is, typically, a consequence of nonlinearity.

The result of our analysis is that these solutions can be classified as two different types, independently of the number of parameters they contain. The generic behavior of these Einstein–Rosen metrics can be worked out through the study of the simplest models.

The first model, studied in Section 4, is the "one-soliton" solution with two parameters only. The most general static solution with cylindrical symmetry is the Levi-Cività metric which can be interpreted as the external field of an infinite cylinder with a well-defined mass per unit length [2]. It is natural to use this solution (seed solution) as the starting point of the inverse scattering transform, and the result can be understood as Einstein–Rosen radiation on a Levi-Cività background. The asymptotic behavior of this simple model is far from satisfactory. However, it is of use to characterize, qualitatively, a model family of the "n-soliton" solutions.

The second model, discussed in Section 5, is a "two-soliton" solution with four parameters and it characterizes the remaining n-soliton solutions. These solutions represent, now, localized soliton waves on a Levi-Cività background, possessing therefore the axial singularity only. We perform, in Section 5, a perturbative analysis of these metrics and show that they are characterized by a pulse-like perturbation, with a characteristic height and width, which propagates at a superluminal velocity. In Section 5 we use the space-time evolution of the optical scalars to gain further insight into the physical properties of these solutions.

An interesting feature of the Einstein–Rosen metrics was discovered by Thorne [3], who was able to define, unambiguously, a localized energy density, the so-called C-energy density. Also in Section 5, we make use of this quantity to draw complementary information about our metrics.

2. THE SEED METRIC

As a first step one usually chooses a simple seed solution. This means, in fact, that we require of the seed more symmetries than are necessary to apply the solution technique. In this case we have choosen an abelian group G_3 with the three Killing vectors ∂_t, ∂_ϕ, ∂_z.

This is, however, too mild a restriction; the general vacuum solution for this symmetry is known [1] and does not posses a clear physical interpretation. Instead of this we restrict ourseles to the static family found by Levi-Cività [7]. This family can be written in the form

$$ds^3 = \beta\rho^{(\delta^2-1)/2}(d\rho^2 - dt^2) + \rho^{\delta+1}\, d\phi^2 + \rho^{1-\delta}\, dz^2 \tag{1}$$

with β and δ arbitrary parameters. This solution plays within the context of cylindrical symmetry the same role that the Schwarzschild solution plays in the spherically symmetric cases.

There is, in general, an infinite line singularity at $\rho = 0$, rather than a point-like one. It is a naked singularity and an event horizon cannot be built to hide it.

This solution was first studied by Levi-Cività, and in the Newtonian limit, he found

$$\delta \simeq \frac{1+2M}{1-2M} \tag{2}$$

where M is the relativitic mass per unit length (GM/c^2R) of a cylinder (R being a characteristic length of the physical problem).

For $M = 0$, $\delta = 1$ and metric (1) is flat space; δ grows without bound when $2M \to 1$. One may take the parameter $\beta = 1$, so that one recovers flat space in standard coordinates when $\delta = 1$ [8]. However, Marder [2], studying the matching problem of (1) with an interior solution for a physical cylinder, assuming a specific equation of state, concluded that in this case β does depend on δ (therefore on the mass density) and cannot be put equal to one. In what follows we shall assume δ and β arbitrary parameters.

Thus, for $\delta > 1$ metric (1) can be interpreted as the exterior field of an infinite cylinder with certain mass per unit length, M.

There is an important difference with the Schwarzchild solution that must be pointed out. The Levi-Cività solution is not the most general exterior solution to a cylinder. Looking at Einstein's equations with (total) cylindrical symmetry one can easily see that gravitational waves can be superimposed on the exterior field of a static cylinder. This is in contrast with spherical symmetry, and will be discussed in the next section.

3. THE EINSTEIN–ROSEN METRICS AND SOLITON SOLUTIONS

The most general metric for gravitational waves in a vacuum, with cylindrical symmetry, was written by Kompaneets [9, 10]

$$ds^2 = e^{2(\gamma-\psi)}(d\rho^2 - dt^2) + \rho^2 e^{-2\psi}\, d\phi^2 + e^{2\psi}(dz + A\, d\phi)^2 \tag{3}$$

with γ, ψ, A depending on t and ρ alone.

By requiring total cylindrical symmetry (i.e., invarance by $\phi \to -\phi$, $z \to -z$) it reduces to the Einstein–Rosen form [11, 12] $A = 0$. These metrics describe gravitational waves, with only one possible mode of polarization (instead of two modes) and they have been widely studied because the equations governing the field ψ are linear. (Besides once ψ is known γ can be found by quadratures only.) So that, in this case, one can superpose linearly the solutions ψ of the field equations.

To the static Levi-Cività background (1) $\psi_b = (1-\delta)/2 \ln \rho$ one may superpose wave solutions $\psi(t, \rho)$. Marder [2] has calculated the effect of pulse waves on particles moving on geodesics and the change in proper mass per unit length of a particular solid cylinder. Thorne [3] found that the decrease of proper mass was equal to the C-energy carried by the waves. The C-energy of our solutions will be studied later.

Here we shall superpose soliton waves on a static cylinder. The general n-soliton solution for the Einstein–Rosen metric

$$ds^2 = f(d\rho^2 - dt^2) + g_{\phi\phi}\, d\phi^2 + g_{zz}\, dz^2 \tag{4}$$

can be obtained by a coordinate transformtion from the diagonal n-soliton solution with the Kasner seed obtained in the cosmological context by Carr and Verdaguer [6] in the canonical coordinates (t, z). These coordinates transform simply to the canonical coordinates (ρ, t) of metric (3), and the solution in the cylindrical context reads

$$g_{\phi\phi} = \rho^2 \exp[-2\psi_b] \exp\left[-2 \sum_{i=1}^{n} \psi_i(t, \rho)\right] \qquad g_{zz} = \rho^2 / g_{\phi\phi} \tag{5}$$

where

$$\psi_i(t, \rho) = -\tfrac{1}{2} \ln \sigma_i$$

with

$$\sigma_i^{\mp} = \frac{w_i^2 + \tau_i^2}{\rho^2} + a_i \mp \sqrt{2}\left[\frac{w_i^2 - \tau_i^2}{\rho^2} + \frac{(w_i^2 + \tau_i^2)^2}{\rho^4} + a_i \frac{w_i^2 + \tau_i^2}{\rho^2}\right]^{1/2}$$
$$a_i \equiv \left[1 + 2\frac{(w_i^2 - \tau_i^2)}{\rho^2} + \frac{(w_i^2 + \tau_i^2)^2}{\rho^4}\right]^{1/2}, \qquad \tau_i \equiv t_i - t \tag{6}$$

with w_i, t_i arbitrary real parameters. The two possible values of σ_i, σ_i^-, and σ_i^+ are related by $\sigma_i^- = (\sigma_i^+)^{-1}$.

The metric coefficient f is obtained by quadratures, once $g_{\phi\phi}$ and g_{zz} are known [4]. The solitonic character of those solutions is attached to the functions $\sigma_i(t, \rho)$, as it will become apparent in the remaining sections. The general properties of metrics (5) will be qualitatively understood by studying the simple solutions with one soliton σ_1, and with two solitons $\sigma_1^- \sigma_2^+$.

4. ONE-SOLITON METRICS

These are the simplest solutions of type (5). They involve two real parameters, only w_1 and t_1; without loss of generality we can take $t_1 = 0$. Its explicit form is, dropping subindices

$$f = \beta \frac{\rho^{(\delta^2-5)/2} \sigma^{\delta+2}}{H(1-\sigma)^2}, \qquad g_{\phi\phi} = \rho^{1+\delta}\sigma, \qquad g_{zz} = \rho^{1-\delta}\sigma^{-1} \tag{7}$$

where

$$H \equiv (1-\sigma)^2 + 16w^2\sigma^2\rho^{-2}(1-\sigma)^{-2}$$

To gain some insight on the properties of these solutions it is useful to study the limits $|t| \ll \rho \to \infty$, $|t| \simeq \rho \to \infty$, $\rho \ll |t| \to \infty$, and $\rho \to 0$.

For $|t| \ll \rho \to \infty$ the function σ, taking the prescription σ^+, is

$$\sigma \simeq 1 + \frac{2w}{\rho}$$

and metric (7) just behaves as the Levi-Cività seed solution (1). The only difference is the value of the parameter in the function f: instead of β one has $\beta/16w^2$.

A similar behavior for the σ function is found in the limit $|t| \simeq \rho \to \infty$ since in this case

$$\sigma \simeq 1 + 2\sqrt{w/\rho}$$

However, the intrinsic properties of the metric are very different from the Levi-Cività solution in this limit. In fact, if we write the Riemann tensor for a metric of type (4)

$$R^{(\alpha\beta)}_{(\gamma\delta)} = \begin{pmatrix} E & B \\ -B & E \end{pmatrix}$$

where E and B are 3×3 matrices, whose only nonzero elements are $E_{11}=e_1$, $E_{22}=e_2$, $E_{33}=-e_1-e_2$ and $B_{12}=B_{21}=b$, the Riemann tensor components in the limit $|t|\simeq\rho\to\infty$ have the leading terms such that

$$e_1\simeq -e_2\simeq b$$

and that is a type N metric in the Petrov classification. That is, on the light cone the family of solutions (7) behave asymptotically as pure gravitational radiation in the canonical coordinates (ρ, t): incoming radiation toward the symmetry axis in the past $t<0$, and outgoing radiation in the future. The amplitude of the radiation is maximal on the light cone $|t|\simeq\rho$, far from the axis.

The limits $\rho\ll|t|\to\infty$ and $\rho\to 0$ can be discussed simultaneously since the respective limits of σ are

$$\sigma\simeq 4\frac{t^2}{\rho^2}[1+0(t^{-1})] \qquad \text{and} \qquad \sigma\simeq 4\frac{w^2+t^2}{\rho^2}[1+0(t^{-1})]$$

and the metric becomes

$$f\simeq\beta 4^{\delta-2}(w^2+t^2)^{\delta-2}\rho^{(\sigma-1)(\delta-3)/2}$$

$$g_{\phi\phi}\simeq\rho^{\delta-1}4(w^2+t^2), \qquad g_{zz}\simeq\rho^{3-\delta}\frac{1}{4(w^2+t^2)} \tag{8}$$

This metric for $|t|\ll w^2$ and $\rho\to 0$ behaves just as a Levi-Cività metric with a new $\delta'\equiv\delta-2$. Special cases are $\delta=1$ $(\delta'=-1)$ and $\delta=3$ $(\delta'=1)$ since in both cases it tends to flat space. A possible interpretation can be given if we look at $t=$ constant $(t=t_c)$ hypersurfaces: the metric near the axis can be seen as a Levi-Cività metric with parameter $\delta'=\delta-2$ and a new parameter $\beta'=\beta 4^{\delta-2}(w^2+t_c^2)^{\delta-2}$. At larger t_c, β' gets larger if $\delta>2$; but the function f^{-1} is proportional to Thorne's C-energy [3] and we can think that the C-energy of the field decreases as t_c grows. This may be related to the energy carried by the waves.

The general picture for those metrics then emerges: take a value for $\delta>3$ and the hyperspace $t>0$, the field in the region $\rho\to\infty$ is close to that of a static cylinder of mass per unit length $M\simeq\frac{1}{2}(\delta-1/\delta+1)$ and with parameter $\beta/16w^2$. Near the axis $\rho\to 0$, it is the field of a cylinder with a mass $M'\simeq\frac{1}{2}(\delta'-1/\delta'+1)$ with $\delta'=\delta-2$ and $\beta'\simeq\beta w^{2\delta'}$. If we take now a hyperspace at large $t=t_c$, in the region $t_c\ll\rho\to\infty$ we will have the field of the cylinder with δ, on the light cone $\rho\sim t_c$, the field is that of pure radiation and at a finite distance from the axis the field is that of a cylinder with mass M' and $\beta'\simeq\beta t_c^{2\delta'}$. Therefore the C-energy $(\sim(\beta')^{-1})$ is now

smaller: the energy has been radiated. In particular if we take $\delta = 3$ the evolution is toward flat space $\delta' = 1$.

This picture is symmetrical for $t < 0$ with incoming radiation.

For metric (7) with prescription σ^- the picture is qualitatively similar but near the axis it is like a Levi-Cività metric with $\delta' = \delta + 2$.

These metrics, however, do not have a clear physical interpretation since their global properties are not physical. Besides the usual axial singularity they are also singular at $|t| \to \infty$.

The qualitative behavior of a metric of the general type (5) can be easily understood now. We write the $g_{\phi\phi}$ component showing explicitly the different prescriptions used for σ_i in (6) as

$$g_{\phi\phi} = \rho^{1+\delta} \prod_{i=1}^{k} \sigma_i^+ \prod_{i=k+1}^{n} \sigma_i^-$$

the asymptotic behavior near the axis is that of a Levi-Cività metric with $\delta' = \delta + 2(n-2k)$ whereas it behaves as the Levi-Cività seed at $\rho \to \infty$.

For $n \neq 2k$ the global properties of these metrics are similar to those described above. However, for $n = 2k$ the soliton metrics tend to the seed Levi-Cività metric in both assymptotic regions and they can be interpreted as localized finite disturbances (soliton like) on the Levi-Cività background. They will be discussed in the next section.

5. TWO-SOLITON METRICS

These metrics are obtained as the linear superposition (in the sense of linear superposition of the field ψ of metric (3)) of two soliton fields on the Levi-Cività static background. They can be written [6] as

$$f = \frac{\rho^{[(\delta^2-17)/2]}}{H_1 H_2} \frac{\sigma_1^\delta \sigma_2^\delta}{(1-\sigma_1)^2(1-\sigma_2)^2} \left\{ \left[(\sigma_1+\sigma_2)\rho^2 - \frac{8\tau_1\tau_2\sigma_1\sigma_2}{(1+\sigma_1)(1+\sigma_2)} \right]^2 - \frac{64 w_1^2 w_2^2 \sigma_1^2 \sigma_2^2}{(1-\sigma_1)^2(1-\sigma_2)^2} \right\}^2 \tag{9}$$

$$g_{\phi\phi} = \rho^{1+\delta}\sigma_1\sigma_2 \qquad g_{zz} = \rho^{1-\delta}(\sigma_1\sigma_2)^{-1}$$

We shall take now the prescription σ_1^- and σ_2^+ with $w_2 \neq w_1$ and, for simplicity, $t_1 = t_2 = 0$.

The product $\sigma_1^- \sigma_2^+$ behaves in the asymptotic region $|t| \ll \rho \to \infty$, like $1 + O(\rho^{-1})$, in the region $\rho \ll |t| \to \infty$ like $1 + O(t^{-1})$, whereas in $|t| \simeq \rho \to \infty$ it goes like $1 + O(t^{-1/2})$. Thus, the maximum deviation from

the static background is localized, asymptotically, in the light cone region. The size, shape, and motion of this perturbation depends on the parameters w_1 and w_2, as the analysis in the next section will show. From the expressions for $g_{\phi\phi}$ and g_{zz} it is apparent that the metric tensor (9) tends to the Levi-Cività metric in the limits $|t| \ll \rho \to \infty$ and $\rho \ll |t| \to \infty$ and this is proved by the asymptotic behavior of the Riemann tensor components in the canonical coordinates. However, in the limit $|t| \simeq \rho \to \infty$ the leading terms of the Riemann components are those of pure radiation, as it is typical of some soliton solutions [13]. Thus one can interprete naturally this metric as a soliton wave on the field of a static cylinder. The localized wave arises as an interference effect resulting from the superposition of two radiating fields of the type studied in the last section.

Perturbative Analysis

A perturbative analysis assuming that $w_1 - w_2 = \delta w$ is small ($|\delta w| \ll 1$) allows one to obtain analytic expressions for the shape and motion of the solitonic perturbation as well as to give a physical meaning to the parameters (w_1, w_2). Since the basic function of metric (9) is $\sigma_1\sigma_2$, because the f coefficient is determined by Einstein's equations in terms of $g_{\phi\phi}$ and g_{zz}, we shall concretize the analysis on this function. If we define $\sigma = \sigma_2$ and $w = w_1$ we can write

$$\sigma_1\sigma_2 \simeq 1 + \delta w\, \partial_w \ln \sigma \tag{10}$$

The right-hand-side perturbation is too complicated in terms of (ρ, t) (see (6)) to find analytic expressions for its shape and motion directly. Instead we shall introduce new coordinates (R, T) depending on w, defined by

$$\begin{aligned} \rho &= w \cosh 2T \sinh 2R \\ t &= w \sinh 2T \cosh 2R \end{aligned} \tag{11}$$

with $(0 \leqslant R < \infty)$ and $(-\infty < T < \infty)$. In terms of these coordinates $\sigma = \tanh^2 R$. From (11) we deduce

$$2w\, \partial_w R = -\sinh 2R \cosh 2R(\cosh^2 2R + \cosh^2 2T - 1)^{-1}$$

and (10) becomes

$$\partial_w \ln \sigma = -2w^{-1} \cosh 2R(\cosh^2 2R + \cosh^2 2T - 1)^{-1}$$

and we can now find the maximum in the ρ direction of this function by solving the equation

$$\partial_\rho \partial_w \ln \sigma = 0 \tag{12}$$

This can be easily done after finding $\partial_\rho R$ and $\partial_\rho T$ from the coordinate change (11). The solution in (R, T) coordinates is

$$3 \sinh^2 2T = \cosh^2 2R$$

It can now be transformed to (ρ, t) coordinates; using $\cosh^2 2T$ and $\cosh^2 2R$ as intermediate coordinates the computations are rather simple. The final result which gives the trajectory of the mximum ρ_m in terms of t is

$$\begin{aligned} \rho_m^2 &= (w + t/\sqrt{3})(\sqrt{3}t - w) \qquad \text{for} \quad t \geqslant w/\sqrt{3} \\ \rho_m^2 &= (t/\sqrt{3} - w)(\sqrt{3}t + w) \qquad \text{for} \quad t \leqslant -w/\sqrt{3} \end{aligned} \tag{13}$$

and for $-w/\sqrt{3} \leqslant t \leqslant w/\sqrt{3}$ is $\rho_m = 0$. Thus the pulse has a maximum on the symmetry axis for $-w/\sqrt{3} \leqslant t \leqslant w/\sqrt{3}$ and at time $|t| > w/\sqrt{3}$ this maximum propagates on the (ρ, t) plane. Thus the parameter $w/\sqrt{3}$ characterizes the time of formation of the pulse (soliton).

The speed of this pulse in terms of (ρ, t) is now found to be

$$d\rho_m/dt = (w + \sqrt{3}t)(3w + \sqrt{3}t)^{-1/2}(\sqrt{3}t - w)^{-1/2} \tag{14}$$

for $t \geqslant w/\sqrt{3}$. For $t < 0$ the expressions can be trivially obtained from the $t > 0$ so we shall not discuss them further. From (14) we see that the speed of the soliton is infinite at the beginning $t = w/\sqrt{3}$ and it tends to unity (the speed of light) when $t \to \infty$. The trajectory of the maximum approaches the asymptotes $\rho = t + w/\sqrt{3}$ for the outgoing pulse and $\rho = -t + w/\sqrt{3}$ for the incoming pulse.

The shape of the pulse, its height h and width Δ, can now be found. The height is defined by

$$h = |\delta w \, \partial_w \ln \sigma(\rho_m)|$$

Using again the intermediate variables $\cosh^2 2T$ and $\cosh^2 2R$, which make the algebraic manipulations become simpler, and then substituting back the (ρ, t) coordinates, we finally get

$$h = \delta w \tfrac{1}{2}(\sqrt{3}w^{-1}t^{-1} + 3\sqrt{3}t^{-2})^{1/2} \tag{15}$$

Thus, initially at $t = w/\sqrt{3}$, $h \sim \delta w/w$, but for large t, $h \sim (\delta w/2)(3\sqrt{3})^{1/2} t^{-1}$, independently of w. The parameter δw characterizes the strength of the pulse and a small w gives a higher pulse initially.

We can now find the width of the pulse. It is defined by $\Delta = |\rho_1 - \rho_2|$ where ρ_1 and ρ_2 are the ρ coordinates where $\delta w\, \partial_w \ln \sigma$ equals $h/2$ (full width half maximum).

The analytic expression for the width is found to be

$$\Delta = \left(\frac{z_2}{w}\frac{|t|}{\sqrt{3}} + 1\right)^{1/2}\left(\frac{|t|\sqrt{3}}{wz_2} - 1\right)^{1/2} - \left(\frac{z_1}{w}\frac{|t|}{\sqrt{3}} + 1\right)^{1/2}\left(\frac{|t|\sqrt{3}}{wz_1} - 1\right)^{1/2}$$

where

$$z_1 \equiv \chi\left[\left(1 - \frac{3}{\chi^2}\right)^{1/2} + \sqrt{2\left(1 - \frac{3}{\chi^2}\right)^{1/2} - 1}\right]$$

$$z_2 \equiv \chi\left[\left(1 - \frac{3}{\chi^2}\right)^{1/2} - \sqrt{2\left(1 - \frac{3}{\chi^2}\right)^{1/2} - 1}\right]$$

and

$$\chi \equiv (4 + \sqrt{15})^{1/3} + (4 - \sqrt{15})^{1/3}$$

Its behavior for large t can be easily computed from the previous expressions

$$\lim_{t \to \infty} \Delta = \frac{1}{2}\left[\left(\frac{z_2}{\sqrt{3}} + \frac{\sqrt{3}}{z_2}\right) - \left(\frac{z_1}{\sqrt{3}} + \frac{\sqrt{3}}{z_1}\right)\right] \simeq 4.87 \tag{16}$$

and it is found to be independent of w.

All the properties of the space-time (9), that is, its curvature and physically associated quantities such as those discussed in the next sections will have a behavior qualitatively similar to the pulse wave discussed here. We can now summarize and comment upon some of those properties.

First we have seen that this pulse propagates at a speed greater than the speed of light and only approaches it asymptotically. Thus the soliton pulse cannot be interpreted as the propagation of a causal effect; it is rather the result of the interference due to the superposition of σ_1^- and σ_2^+ by means of which different parts of the space-time get localized perturbations at different times.

Although there is no definition of a soliton in General Relativity, these pulse waves have features similar to the classical solitons such as in hydrodynamics. The classical solitons are characterized by being localized

perturbations of constant amplitude, with some characteristic speed of propagation, that emerge basically unmodified after collisions. Here we see that they are localized perturbations and have a characteristic speed of propagation. Although their amplitude decreases with time this must be understood as a consequence of being localized at a larger radius as time increases. Their width, however, becomes constant at large times. The properties of these perturbations under collisions cannot be studied in the two-soliton solution, we need at least the four-soliton solution. In the cosmological context it has been shown, in [13], that the cosmological solitons emerge unmodified after scattering. Such conclusions can be translated easily into the cylindrical context after a coordinate change.

Optical Scalars

To analyze further those solutions and, in particular, their "solitonic" character it is convenient to study the optical parameters associated to a null congruence. The interest is twofold: on the one hand, the Einstein–Rosen metric admits a preferred vector field associated to geodesic null congruences. Therefore an invariant characterization of the metric can be done by the expansion, θ, shear, σ, and rotation, ω ($\omega = 0$ for these metrics) associated to the null congruence. On the other hand, the shear and expansion produced by the solitons on the null rays give physical information about these waves and measure, in some way, the energy carried by them.

The expansion and shear are given by $\theta = (1/2\sqrt{2})(1/f\rho)$ and

$$\sigma = \delta\theta - \frac{1}{2\sqrt{2}} \frac{1}{f} [(\ln \sigma_1 \sigma_2)_{,t} + (\ln \sigma_1 \sigma_2)_{,\rho}]$$

To explore their behavior we shall use the congruence of null rays, defined by

$$t = \rho + c \tag{17}$$

where c is an arbitrary parameter ($-\infty < c < \infty$) (Fig. 1). We shall give the optical scalars in terms of the affine parameter λ defined by

$$\lambda = \int f(\rho + c, \rho)\, d\rho \tag{18}$$

The reason for using the affine parameter is its physical meaning. For the Minkowski metric, the seed metric with $\delta = 1$, it is $\lambda \sim \rho$ (there is always an arbitrary multiplicative factor) and therefore $\theta \sim 1/\lambda$ so that λ can be interpreted as the "parallax" distance from the symmetry axis [14].

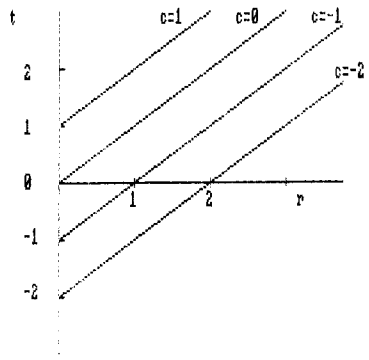

Fig. 1. Null geodesics $t = c + \rho$ used to study the behavior of the optical scalars.

For a massive cylinder $\lambda \sim \rho^{(\delta^2+1)/2}$ and $\theta \sim 1/\lambda$ as before, therefore one can again interpret λ as the parallax distance from the axis that would be defined by a local observer measuring θ. Since metrics (9) represent some finite perturbations on the background field of a cylinder it seems reasonable to compare the expansion and shear of congruences (10) with those of the background: θ_b, σ_b.

In Figs. 2–5 the ratios $\theta(\lambda, c)/\theta_b(\lambda, c)$ and $\sigma(\lambda, c)/\sigma_b(\lambda, c)$ are represented. Those ratios are almost unity everywhere except in the regions where the null ray "hits" the interference region where they get expanded and distorted. For the null ray with $c = 0$ those ratios are different from unity

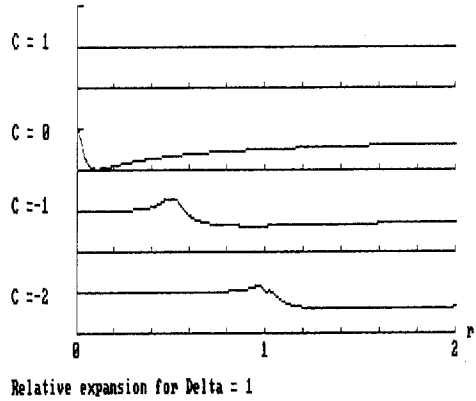

Fig. 2. Relative expansion in arbitrary units, for $\delta = 1$, shown as a function of r. Each curve shows the deviation from 1 along the null geodesics defined by the values $c = 1, 0, -1, -2$. The maximum deviation is found where the null ray hits the soliton (for $c = -1, -2$), or when it moves in the same direction ($c = 0$).

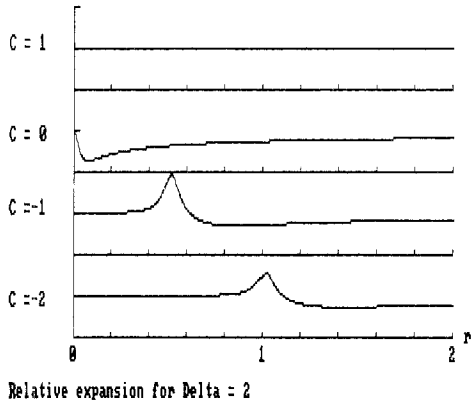

Fig. 3. Relative expansion in arbitrary units for $\delta = 2$.

everywhere, indicating that the interference region is localized near the null cone and they approach unity as $\lambda \to \infty$ because the interference amplitude also decreases in this limit. The solitonic (localized) character of the wave is clearly seen from those diagrams. The localization of the disturbance is governed by the parameters w_1 and w_2, the smaller their difference the more localized the disturbance is.

To understand how the energy carried out by the wave has modified the source we can turn now to Thorne's C-energy.

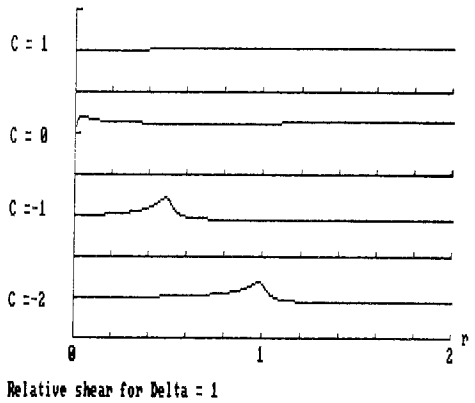

Fig. 4. Relative shear in arbitrary units for $\delta = 1$. The same null geodesics have been used to study its behavior. The qualitative results are the same.

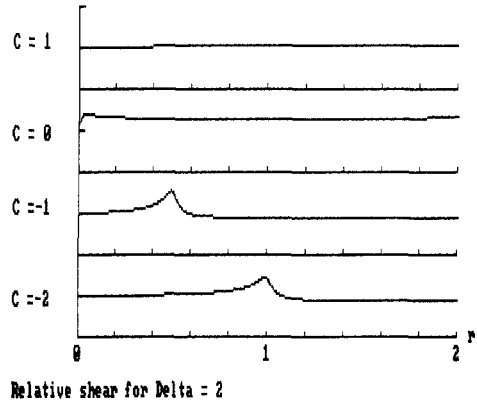

Fig. 5. Relative shear in arbitrary units for $\delta = 2$.

Energy Density Analysis

Although metrics with cylindrical symmetry are not asymptotically flat, Thorne [3], was able to define a total energy, called C-energy, for those systems. In fact, one can define a contravariant C-energy flux vector P^α obeying a conservation law $P^\alpha_{;\alpha} = 0$. The energy density is localizable and locally measurable. Near the axis of a static cylinder it reduces to the proper mass of the cylinder. Such energy is also propagated by Einstein–Rosen gravitational waves. It is thus a very useful quantity [15].

The key function from which the C-energy is defined is the potential C-energy function, which in our coordinate system reads $E \equiv (4G)^{-1}\gamma$, where $\gamma(\rho, t)$ is defined in (3).

It is interesting to note that for a solid cylinder considered by Marder [2] the change in proper mass per unit proper length, when it emits a gravitational wave pulse, is precisely $E_{\text{wave}} = E_{\text{after}} - E_{\text{before}}$; which is also the total C-energy per unit standard length carried away by the wave pulse [3]. This can also be computed in our solutions (9) evaluating E for some fixed radius ρ (large) at $t = 0$, before the passage of the wave, and after at $t \to \infty$. In both cases the metric tends to the static background but with a different coefficient β.

The explicit result is

$$E_{\text{wave}} \simeq \frac{1}{4G} \ln \left[\frac{16 w_1^2 w_2^2}{(w_1 - w_2)^4} \right]$$

Thus the passage of the wave has permanently affected the gravitational field: energy has been radiated away.

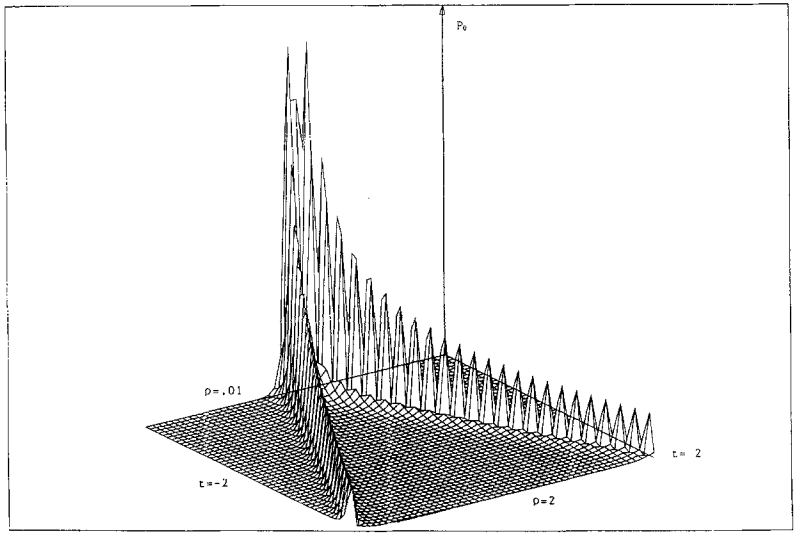

PLOT OF PO IN THE RANGE T=-2, 2 R=.01, 2 D=1

Fig. 6. Plot of the energy density $P^0(t, \rho)$ in arbitrary units ($\delta = 1$). The metric parameters used have been, $w_1 = 0.05$, $w_2 = 0.1$. The soliton is localized near the light cone centered at $t = 0$.

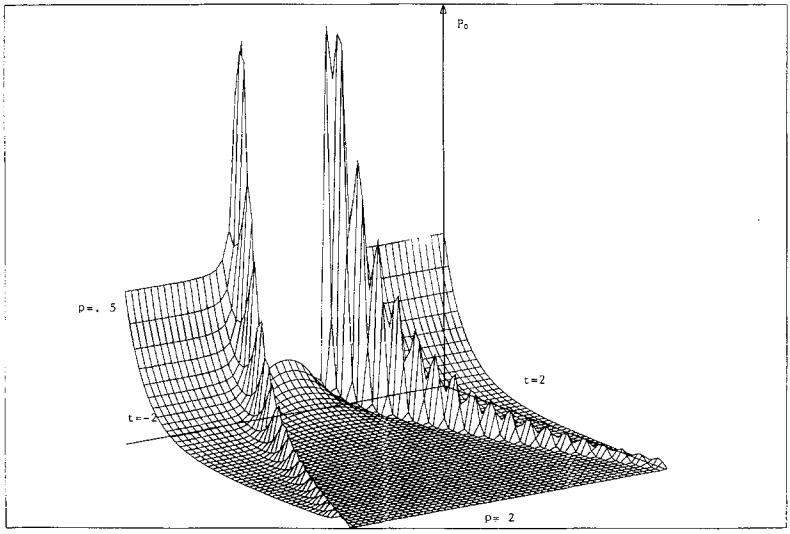

PLOT OF PO IN THE RANGE T=-2,2 R=.5,2 D=2

Fig. 7. Plot of the energy density $P^0(t, \rho)$ in arbitrary units ($\delta = 2$). This corresponds to a massive cylinder ($M = 1/6$). The qualitative behavior is similar to the flat background case, with the exception of the growth of P^0, as we approach the axis, due to the presence of the mass singularity.

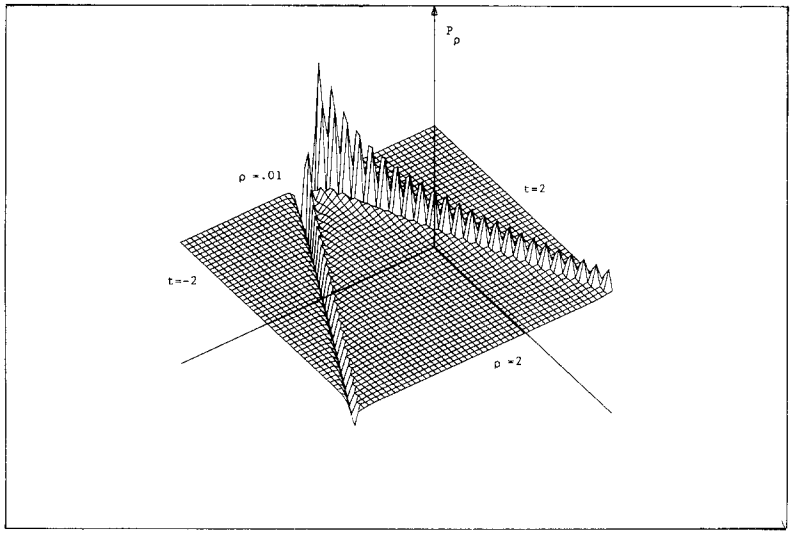

Fig. 8. Energy flux in the ρ direction, $P^{\rho}(t, \rho)$, in arbitrary units for $\delta = 1$. The energy flux is negative for $t < 0$, and positive for positive t. The flat surface of the plot means zero flux.

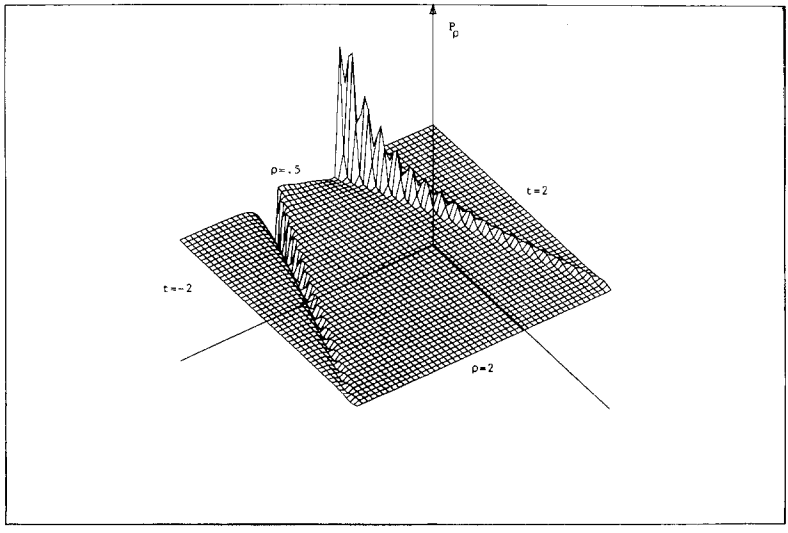

Fig. 9. Energy flux in the ρ direction, in arbitrary units. This corresponds to $\delta = 2$, i.e., $M = 1/6$. The flux is found to increase near the axis although it is null for the static background.

An interesting picture emerges from a quantitative evaluation of the energy density P^t and the energy flux P^ρ defined [3] by

$$\begin{pmatrix} P^t \\ P^\rho \end{pmatrix} \equiv \frac{1}{2\pi\rho^{(\delta+1)/2} f} \begin{pmatrix} \dfrac{\partial E}{\partial \rho} \\ -\dfrac{\partial E}{\partial t} \end{pmatrix}$$

These quantities represent the local energy density measured by a local observer with velocity (1, 0, 0, 0) and the local flux measured by that observer along the ρ direction. Those quantities have been plotted in Figs. 4 and 5. As expected they are localized near the light cone as the disturbances of the optical scalars were.

The computations are made for a flat background and a massive cylinder. Note that when we have a flat background an observer at a certain fixed ρ will see at $t \to -\infty$ a flat space with $\delta = 1$ and $\beta = 1$. However at $t = 0$, when the perturbation is concentrated on the axis, the observer will see a static Levi-Cività field with $\delta = 1$ but $\beta(w_1, w_2) \neq 1$. This is the effect due to the "incoming" energy, in agreement with the above analysis. At $t \to \infty$ the $\beta = 1$ value is restored.

The localized aspect of the perturbation, that is clearly displayed in Fig. 4, suggests that a propagation velocity be defined for it, and it be interpreted as a localized energy density propagating through the space-time. A natural definition for its propagation velocity is the one of the maximum. However, it turns out that this interpretation cannot be sustained because this velocity is greater than one, as the perturbative analysis of Section 5a indicates. Therefore what we are seeing is merely a superluminal effect due to the interference of σ_1^- and σ_2^+.

REFERENCES

1. Kramer, D., Stephani, H., MacCallum, M., and Herlt, E. (1980). *Exact Solution of Einstein's Field Equations* (Cambridge University Press).
2. Marder, L. (1958). *Proc. Roy. Soc. (London)*, **A244**, 524; (1969) **A313**, 83.
3. Thorne, K. S. (1965). *Phys. Rev.*, **B138**, 251.
4. Belinskii, V. A., and Zakharov, V. E. (1978). *Sov. Phys. JETP*, **48**, 985.
5. Belinskii, V. A., and Zakharov, V. E. (1980). *Sov. Phys. JETP*, **50**, 1.
6. Carr, B., and Verdaguer, E. (1983). *Phys. Rev.*, **D28**, 2995.
7. Levi-Cività, T. (1919). *Rend. Acc. Lincei*, **28**, 3.
8. Wilson, W. (1920). *Phil. Mag.*, **40**, 710.
9. Kompaneets, A. S. (1958). *Sov. Phys. JETP*, **7**, 659.

10. Jordan, P., Ehlers, J., and Kundt, W. (1960). *Akad. Wiss. Mainz Abk. Math.–Nat. Kl. Jahrg.*, No. 2.
11. Beck, G. (1925). *Z. Physik*, **33**, 713.
12. Einstein, A., and Rosen, N. (1937). *J. Franklin Inst.*, **223**, 43.
13. Ibáñez, J., and Verdaguer, E. (1983). *Phys. Rev. Lett.*, **51**, 1313.
14. Sachs, R. (1961). *Proc. Roy. Soc. (London)*, **A264**, 309.
15. Piran, T. (1979). *Sources of Gravitational Radiation*, L. Smarr, ed. (Cambridge University Press).